UNIVERSITY OF CALIFORNIA
SANTA CRUZ

**The Vital Balance Between Pre-mRNA Load and Splicing Capacity**

A dissertation submitted in partial satisfaction of the requirements for the degree of

MASTER OF SCIENCE

in

MOLECULAR, CELL & DEVELOPMENTAL BIOLOGY

by

**Michelle Seiwald**

June 2023

The dissertation of Michelle Seiwald is approved by:

_____
Dr. Manuel Ares Jr.

_____
Dr. Melissa Jurica

_____
Dr. Grant Hartzog

_____
Peter Biehl, Dean of Graduate Studies

# Table of contents

# List of figures/tables

**The Vital Balance Between Pre-mRNA Load and Splicing Capacity**

**Michelle Seiwald**

## Abstract

The spliceosome, a large macromolecular machine that removes introns from pre-mRNA to form mature mRNA, contains five small RNAs that play key roles. To learn more about the role played by one of these, U2, we started with a temperature-sensitive mutant of U2, *U33Δ*. Using *U33Δ,* we analyzed secondary mutations that restored growth at a non-permissive temperature in *Saccharomyces cerevisiae*. We found that this suppressor mutation was in a gene, *NOB1,* that is unrelated to splicing and instead is a crucial component of ribosomal RNA processing. This mutation, found to be a delta (δ) insert from a Ty transposable element, causes reduced function in Nob1 and an accumulation of unprocessed rRNA. RNA sequencing revealed *U33Δ* has a splicing defect and change in gene expression, both of which the *nob1-Tyδ* allele restored. How this rRNA processing defect rescues a spliceosome mutant led us to investigate this phenomenon through the lens of systems biology, and we found that decreasing the load of pre-mRNAs or increasing the capacity of the spliceosome were both able to restore the growth of *U33Δ*. We found new mechanisms that can change the pre-mRNA pool that rescue mutations in the spliceosome, adding evidence to the hypothesis that splicing regulation is directly related to the spliceosome's capacity and workload.

# Acknowledgment

Thank you so much to Manny Ares, my advisor, who has been fantastic to work with and is the number one homie. Thank you also to Grant Hartzog for his generous support and help during my undergrad, without which I probably wouldn't have pursued a Master's degree. Thank you to him and Melissa Jurica for their help and support with this thesis. Finally, thank you to Jason Talkish for his collaboration with this project and his excellent work with the analysis of the RNA sequencing data.

# 1 - Introduction

Pre-mRNA splicing is an essential step in gene expression that can create multiple distinct mRNA products from a single gene. Splicing is the removal of introns and the joining of exons in a highly regulated and precise manner. In eukaryotes, the machinery responsible for this process is a dynamic macromolecular complex called the spliceosome. The spliceosome comprises various protein splicing factors and five small nuclear RNAs (snRNAs). One of the essential steps of spliceosome formation is the recognition of the intron branch point via the snRNA U2, which forms the pre-spliceosome. This step in spliceosome formation is critical as it determines whether a pre-mRNA substrate will be spliced and the location of the 3' splice site. Despite its importance, this step in spliceosome formation remains poorly understood. This project initially set out to investigate the interactions of U2 and the intron with other splicing factors where the branchpoint-interacting stem-loop (BSL) within U2 plays a crucial role.

Within U2, the BSL is responsible for contact with the branchpoint within the intron. The structure of the BSL was first proposed as a mechanism for how U2 presents the nucleotides that contact the intron (Perriman and Ares 2010), and in the CryoEM model of human U2 snRNP, this structure appears as a stem-loop (Zhang et al. 2020). The current model predicts that if the branchpoint sequence has acceptable pairing with the loop nucleotides of the BSL, then the BSL unwinds. This process is mediated by the ATP-dependent removal of Cus2 via the DEAD-box RNA helicase Prp5 (Perriman and Ares 2010). The downstream side of the BSL then pairs with the intron to form an extended helix, pairing to the sequence upstream of the intron branch point (Plaschka et al. 2018) (Figure 1).

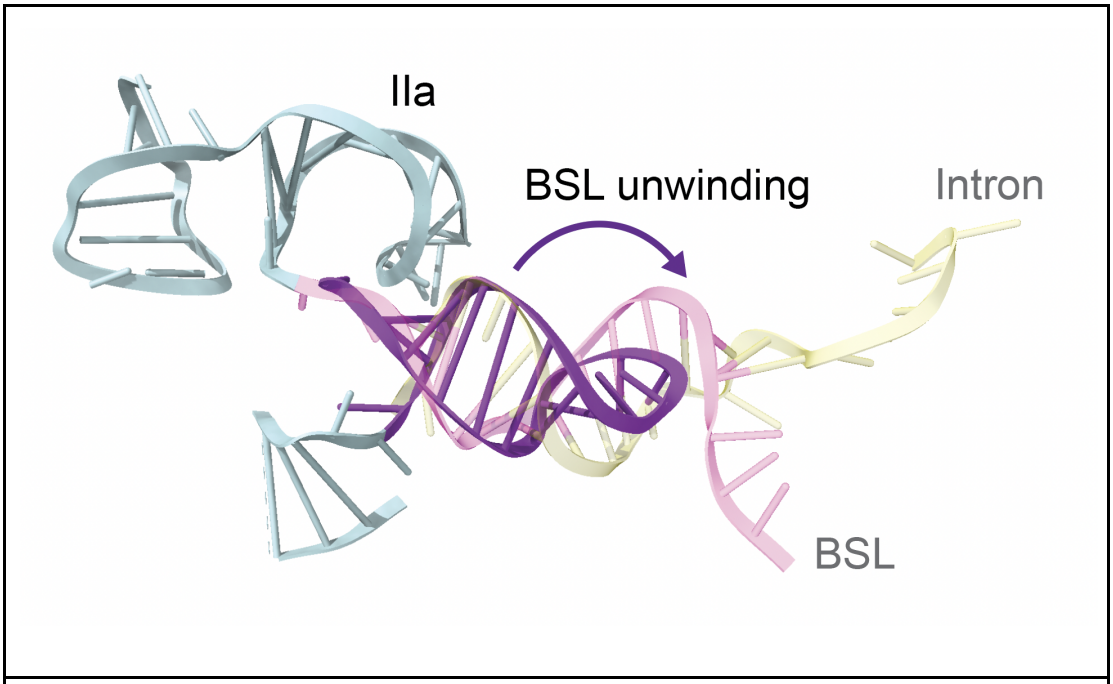


**Figure 1: The BSL is a dynamic structure.** The BSL undergoes structural changes during spliceosome assembly, unwinding from a stem-loop (magenta) to form an extended helix with the intron (lilac and yellow). PDB: 6Y5Q (Zhang et al. 2020), 6G90 (Plaschka et al. 2018)

This step is critical for splicing as it is where the branchpoint is either accepted or rejected, but it is unknown how the BSL transitions between these two states and what criteria must be met for acceptance of the branch point and commitment to the rest of spliceosome assembly. Investigating these mechanisms is critical for understanding how the spliceosome chooses what pre-mRNAs get spliced, which can significantly impact the cell when such mechanisms malfunction.

The stem-loop of the BSL has notable incomplete base pairing, thought to be due to its dynamic structure. This structure requires both the stability needed to function as a stem-loop during branchpoint recognition and the instability to unwind to form the extended helix with the intron (Perriman and Ares 2010). The BSL is a highly conserved sequence across

eukaryotes, indicating the significance of its specific sequence. Despite this, in *Saccharomyces cerevisiae,* previous studies have shown that many mutations in the BSL have no distinct phenotype (Yan and Ares 1996). However, some mutations that disrupt base-pairing have temperature-sensitive phenotypes, while mutants that hyperstabilize the stem-loop by creating new base pairs are cold-sensitive (Yan and Ares 1996). These mutants show that the specific bases may not be as significant as the pairing interactions they create within the stem-loop. These mutants are hypothesized to cause a splicing defect by being unable to remain as a stem-loop long enough to properly contact the branchpoint at high temperatures, in the destabilized mutants, or be unable to unwind to form the extended helix at lower temperatures, in the hyperstabilized mutants.

This thesis focuses on characterizing a suppressor mutation of a mutation in the BSL where U33 is deleted (U33Δ). This mutation causes a destabilization of the BSL (Figure 2). U33 normally pairs with A39, and deletion of U33 causes a temperature-sensitive phenotype (no growth at 37°C). By looking at suppressor mutations, we hoped to discover other factors that influence the recognition of the intron branch point and the subsequent steps that result in the formation of the spliceosome complex, as such factors would likely interact with the BSL or other related spliceosome components to counteract the destabilization. To our surprise, a mutation in Nob1, a protein with no direct link to the spliceosome, was found to suppress this BSL mutation. Investigating the mechanism of action of this *NOB1* mutation led us to look at splicing mechanics through a systems biology lens. While the spliceosome has been heavily studied using genetics, biochemistry, and structural biology, this thesis illustrates how the spliceosome functions within the context of other cellular processes.

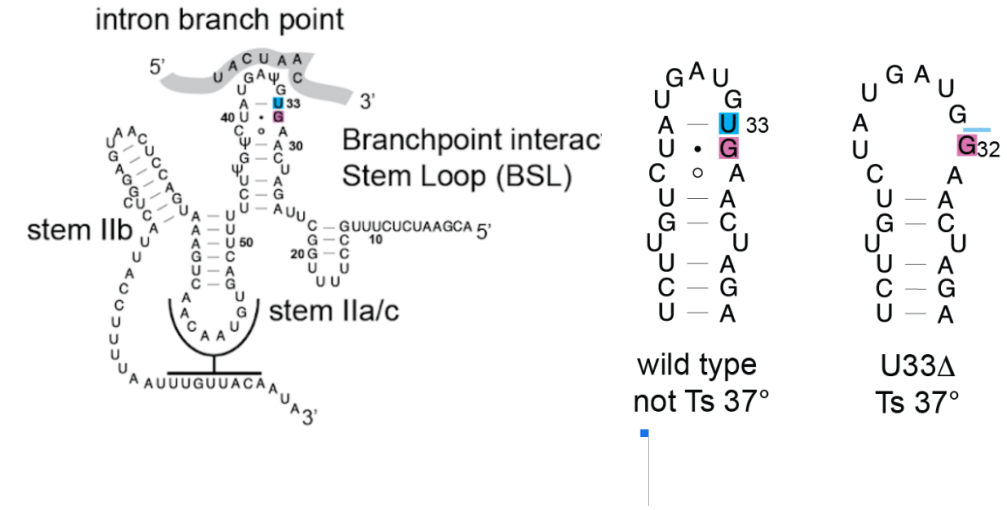


**Figure 2: The structure of BSL is linked to its functional properties.** The BSL contacts the intron branch point. Deletion of U33 disrupts base-pairing of the stem-loop, causing a temperature-sensitive phenotype at 37°C.

# 2 - Characterizing a suppressor of U2 mutant *U33Δ*

Previously, the *NOB1* suppressor mutation was found using a strain with a lethal deletion of U2 (*LSR1Δ)* covered by a plasmid with the U2 allele *U33Δ*. This suppressor arose spontaneously and was determined to be extragenic from *U33Δ* via a plasmid shuffle. When a new plasmid with *U33Δ* was shuffled into the suppressor cells, they still grew at non-permissive temperatures indicating the suppressor mutation was not within the U2 gene. By further characterizing this suppressor, we aimed to identify another factor involved in splicing that interacts with the BSL by understanding the mechanism of its suppression of *U33Δ*.

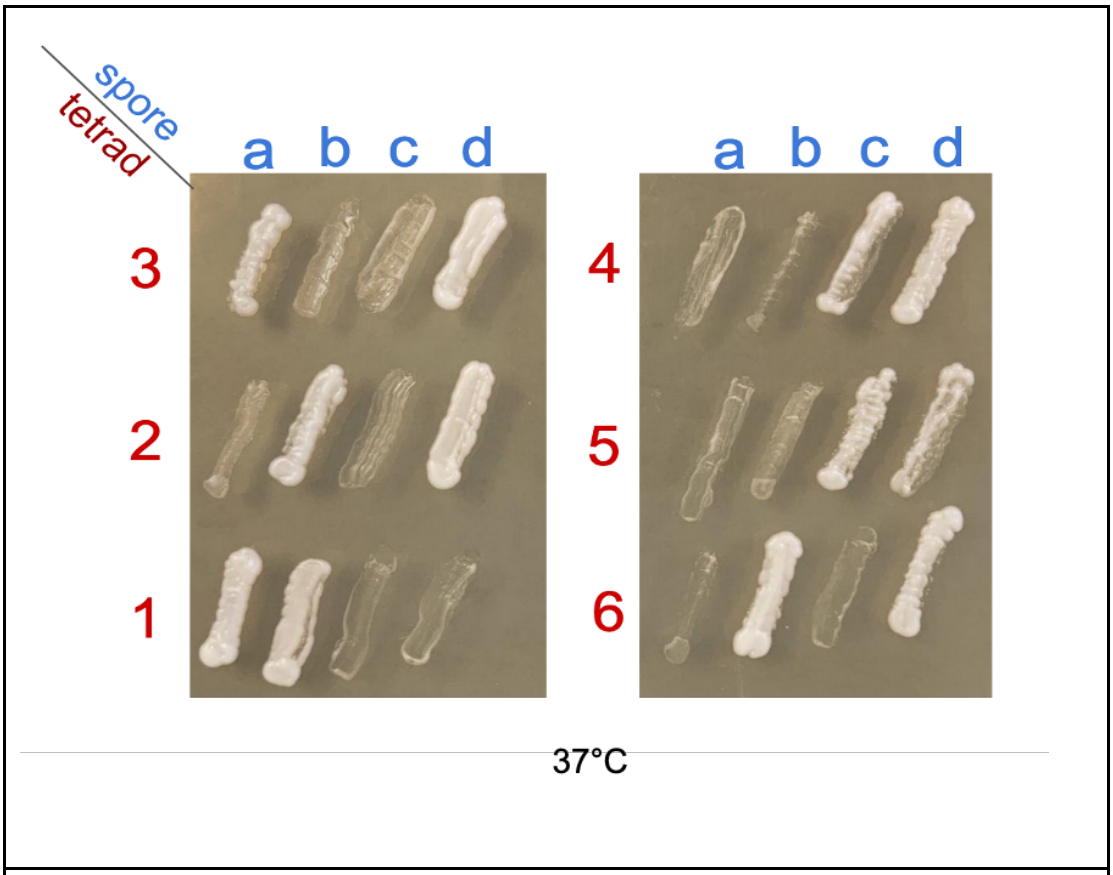


**Figure 3: Suppression of *U33Δ* occurs by a spontaneous mutation in a single gene.** Tetrad spores from a backcross of the suppressor strain grown at non-permissive temperature show 2:2 segregation, indicating suppression via a single, extragenic gene.

The suppressor strain was subjected to a backcross to determine whether the suppression was caused by a mutation in a single gene. The suppressor haploid yeast strain was mated to a non-suppressor haploid strain, both with *U33Δ*, followed by a dissection of tetrads to examine gene segregation. The results of the backcross indicated that a single gene, rather than multiple genes, was responsible for the observed suppression. We observed 2:2 segregation of the suppressor phenotype, as half of the cells survived when grown at non-permissive temperature. This indicates the surviving cells received the gene containing the suppressor mutation, while the non-surviving cells received the wildtype gene from the other

parent utilized in the backcross. The cross also showed the suppressor mutation was recessive, as the diploid parental cells did not grow at 37°C.

The suppressor strain's genomic DNA was sequenced to determine the location of the suppressor mutation in the genome. Genomic DNA was extracted from the six suppressed spores and the six non-suppressed spores from three of the tetrads shown above, pooled into two samples for suppressor and non-suppressor, and these two pools were sequenced and mapped to the yeast genome. A coverage break (a location in the wild-type genome that reads from the suppressor spores fail to cross) was identified in the suppressor spore pool (Figure 4), indicating a mutation different from a single point mutation. This break mapped to the 3' end of the gene *NOB1*, whose protein is involved in ribosomal RNA processing. Such a coverage break could result from an entire translocated sequence normally found elsewhere in the genome but here is present in *NOB1*. A Ty element insertion, a transposable element common across the yeast genome, might explain these results.

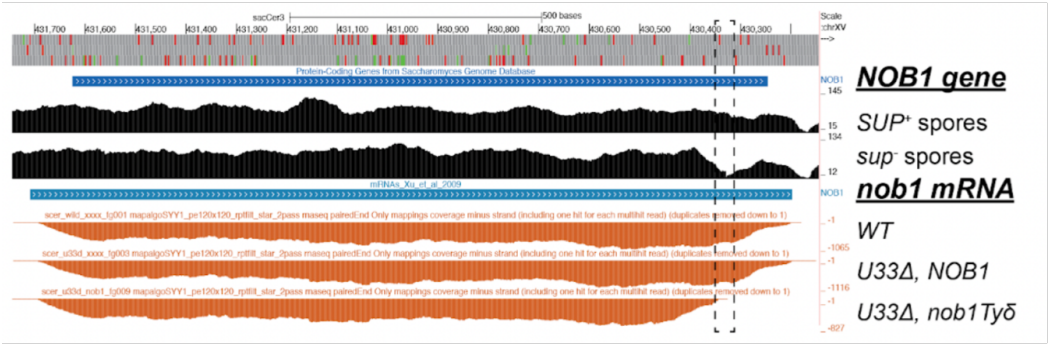


**Figure 4: Suppressor sequencing reveals a coverage break in *NOB1*.** Black is DNA sequencing coverage tracks, while orange is RNA sequencing. Spores that grow at 37°C have a break in coverage in *NOB1*, indicating a sequence mapping elsewhere in the genome.

Colony PCR of the suppressor compared to non-suppressor spores confirmed the

location of the suppressor mutation (Figure 5). Primers flanking the 3' end of *NOB1* were used, resulting in an insert 324bp in length only in the suppressor spores, indicating that the insert was inseparable from the suppressor mutation.

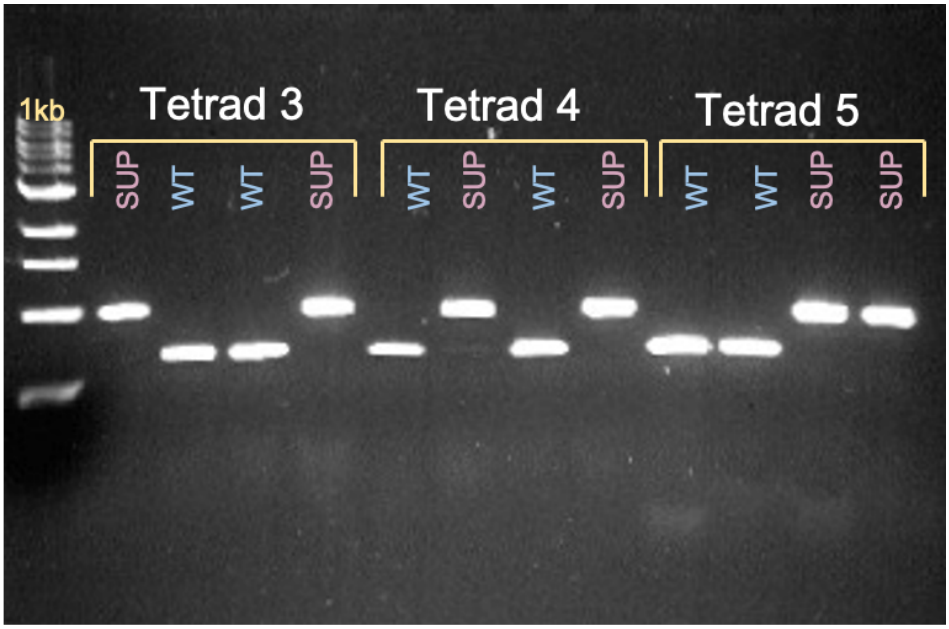


**Figure 5: PCR confirms Ty delta element in the 3' end of *NOB1*.** An insert of approximately 300bp in *NOB1* corresponds to suppression of *U33Δ* temperature sensitivity. Sequencing confirmed the insert was a Ty delta.

This insert was sequenced and shown to be a solo delta (δ) sequence from a Ty transposable element. The nucleotides coding for this 324bp delta resulted in a sequence of amino acids derived from a noncoding part of Ty that replaced the C-terminal end of Nob1. Twenty-eight of Nob1 C-terminal amino acids are substituted in the mutant before it is terminated by a fortuitous stop codon within Ty (Figure 6). The mutation was recreated in a new strain, using CRISPR/Cas9 to insert an identical Tyδ element into *NOB1*. This strain also suppressed *U33Δ* temperature sensitivity, confirming the Tyδ is responsible for the suppression. Our next goal was to determine the mechanism of suppression.

Nob1 has not been shown to have any role in splicing. Previous work has demonstrated that Nob1 is an endonuclease that functions in ribosomal RNA processing of the 40S subunit, where it cleaves 20S rRNA to create 18S rRNA (Fatica et al. 2003). This is a crucial step in the formation of functional ribosomes, and *NOB1* is an essential gene in *S. cerevisiae*. The C-terminal end of Nob1 guides the rRNA into the catalytic PIN domain for this processing (Ameismeier et al. 2018), and so the replacement of the 3' end of *NOB1* with Tyδ was hypothesized to interfere with this function.

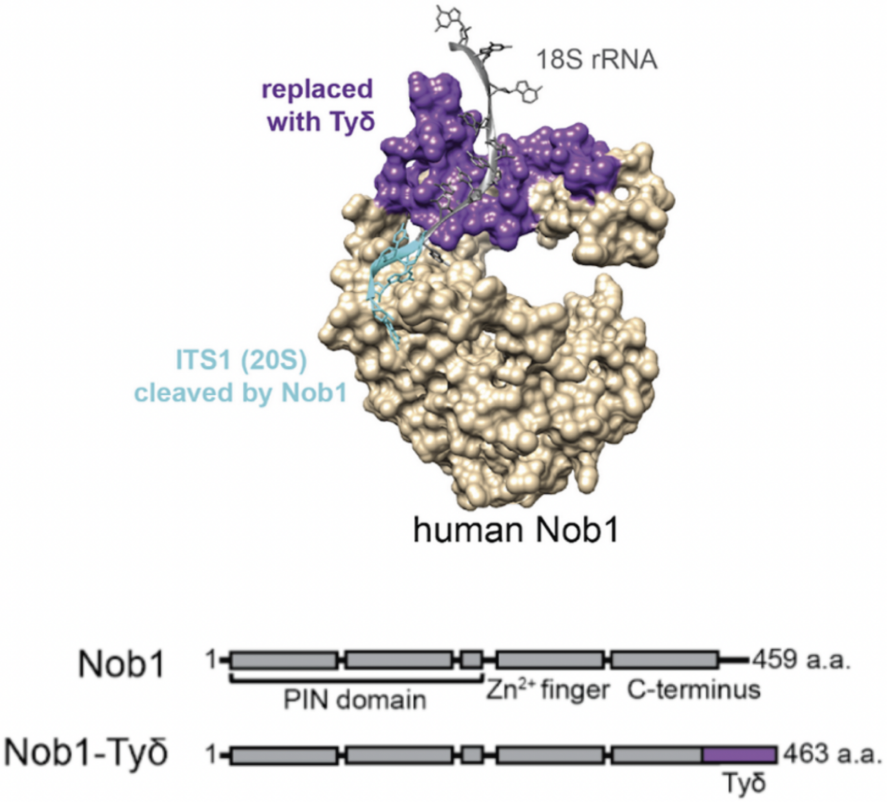


**Figure 6: A Tyδ replaces the C-terminal end of Nob1**. Purple indicates the amino acids in Nob1 replaced by the delta sequence's amino acids. The C-terminal end of Nob1 guides the 20S rRNA to the catalytic site. PDB: 6G4S (Ameismeier et al. 2018)

To test whether the Tyδ interfered with this function, RNA was extracted and analyzed from cells carrying *U33Δ* with either the *NOB1* allele or *nob1-Tyδ,* grown at permissive and non-permissive temperatures (Figure 7). As predicted, rRNA processing was reduced in *nob1-Tyδ*. Though processed 18S is present, there is unprocessed 20S accumulating in *nob1-Tyδ*, with no difference observed between permissive and non-permissive temperatures. A complete block on rRNA processing was not expected since Nob1 and its processing of 20S rRNA is essential for cell survival (Fatica et al. 2003).

Additionally, rRNA processing was tested with a truncated form of Nob1, created using CRISPR/Cas9. This version of Nob1 was created to test whether the Tyδ was significant or simply the lack of the proper C-terminal end of Nob1. In this mutant, two stop codons cause truncation of the C-terminal end of Nob1 at the location where the Tyδ insert begins. This truncation surprisingly did not suppress *U33Δ* (Figure 8), and the processing defect of 20S was also not present (Figure 7). This indicates that the suppression is specifically caused by the Tyδ insert, perhaps caused due to steric effects (Figure 6), and the 20S processing defect is linked to suppression. Diploid *NOB1/nob1-Tyδ* cells were also tested and showed minimal processing defect, reconfirming that *nob1-Tyδ* is recessive.

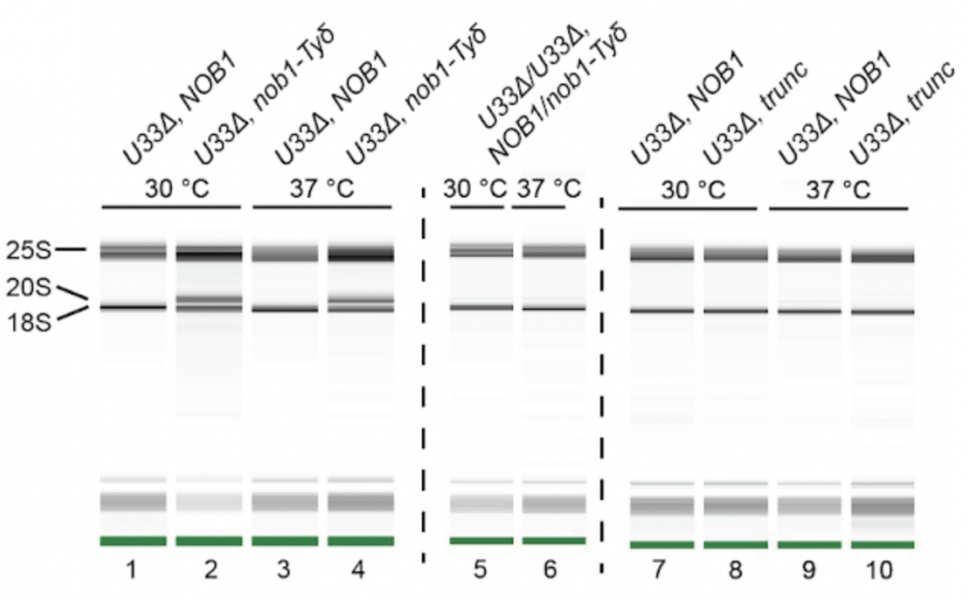


**Figure 7: *nob1-Tyδ* is defective for 20S rRNA processing.** Cells were grown at 30°C and 37°C but showed no difference in processing between temperatures. rRNA processing with *nob1-Tyδ* was compared in haploid and diploid cells, and the truncated Nob1 mutant was shown not to have the processing defect.

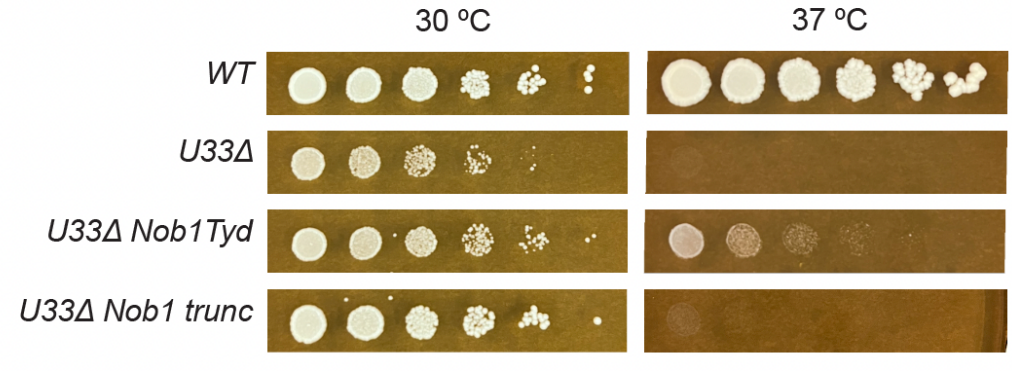


**Figure 8: Truncation of *NOB1* does not cause suppression.** A stop codon that truncates *NOB1* where the Tyδ begins in the suppressor strain fails to rescue *U33Δ* at 37°C.

Next, the *nob1-Tyδ* mutation was tested for allele specificity. Although it suppresses one BSL mutant, we wanted to see whether the same effect could be observed for other temperature or cold-sensitive mutants in the BSL. This would indicate that the suppression is not specific to a certain BSL mutant but is a more general suppressor. Indeed, by shuffling in other U2 mutants on plasmids, we observed that several BSL mutants grew better at non-permissive temperatures with the *nob1-Tyδ* allele compared to *NOB1* (Figure 9). *A31G* and *C41U* are hyperstabilizing cold-sensitive mutants that have reduced growth at 18 ℃ but show improved growth with *nob1-Tyδ*. We concluded that *nob1-Tyδ* is a general suppressor of U2 BSL mutants.

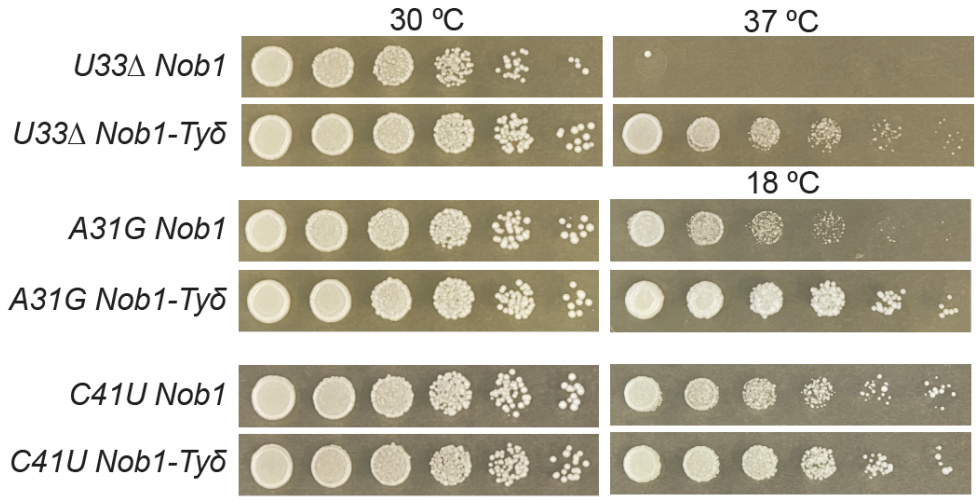


**Figure 9: The *nob1-Tyδ* allele suppresses other mutations in the BSL.** *A31G* and *C41U* are hyperstabilizing cold-sensitive mutants that have reduced growth at 18 °C. *nob1-Tyδ* improves growth at non-permissive temperatures.

Though the mutation causing suppression of *U33Δ* was identified, the precise mechanism and how it related to splicing remained unclear. Using RNA sequencing, we

looked at the genome-wide effects of *U33Δ* and the suppressor *nob1-Tyδ* on splicing and gene expression compared to the wild-type. We sequenced RNA from cells containing *U33Δ* with *NOB1*, *U33Δ* with *nob1-Tyδ*, wild-type U2 with *nob1-Tyδ*, and wildtype. When we compared splicing efficiency between the strains, we found that *U33Δ* exhibits significantly reduced splicing activity compared to the wild-type, indicating *U33Δ* causes a splicing defect (Figure 10). The splicing activity of *nob1-Tyδ* alone is comparable to that of the wild-type, but the mutant *nob1Tyδ* results in a marked improvement in splicing in the *U33Δ* mutant. In this double mutant, the splicing pattern is more evenly matched with the wild-type, indicating partial rescue of the splicing defect for *U33Δ* by *nob1-Tyδ*.

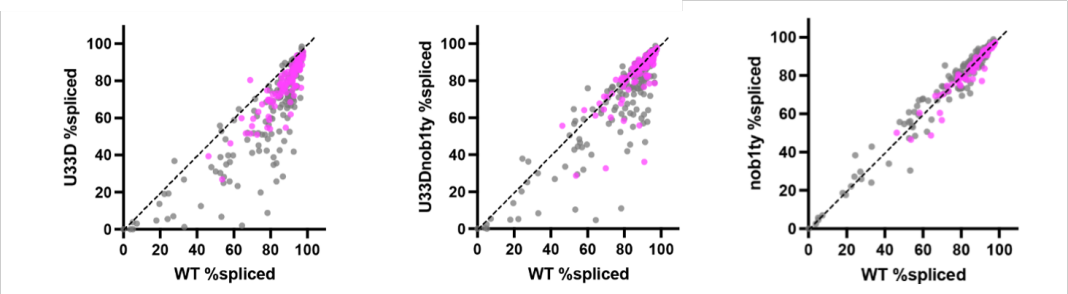


**Figure 10: *U33Δ* has a splicing deficit that is partially restored by *nob1-Tyδ*.** Percent spliced introns of intron-containing genes are shown for *U33Δ*, *U33Δ nob1-Tyδ*, and *nob1-Tyδ* compared to wild-type. Pink indicates ribosomal protein mRNAs.

Then from the RNA sequencing, we analyzed the changes in gene expression levels between *U33Δ* with *NOB1*, *U33Δ* with *nob1-Tyδ*, wild-type U2 with *nob1-Tyδ*, and wild-type. We compared the average transcripts per million versus the change in transcripts per million between the mutants and wild-type, allowing us to see overall trends in changes to gene expression (Figure 11). By looking at transcripts per million, we could visualize the

most dramatic changes to expression. The *U33Δ* mutant exhibited downregulation of gene expression which was restored by the suppressor, trending towards the wild-type expression levels.

Previous findings on the ribosome biosynthesis pathway found that disruption of the pathway causes a down-regulation feedback loop for RPG expression (de la Cruz et al. 2018). Since Nob1 plays a crucial role in rRNA maturation and Nob1-Tyδ has lowered functionality of 20S processing, we thought RPG expression would be decreased. Instead, the *nob1-Tyδ* had an unexpected increase in RPG expression. Likewise, *U33Δ* has a decrease in RPG expression that is restored in the double mutant. We currently lack a clear understanding of this, but this finding is consistent with our hypothesis that the suppressor compensates for the defects caused by the mutation.

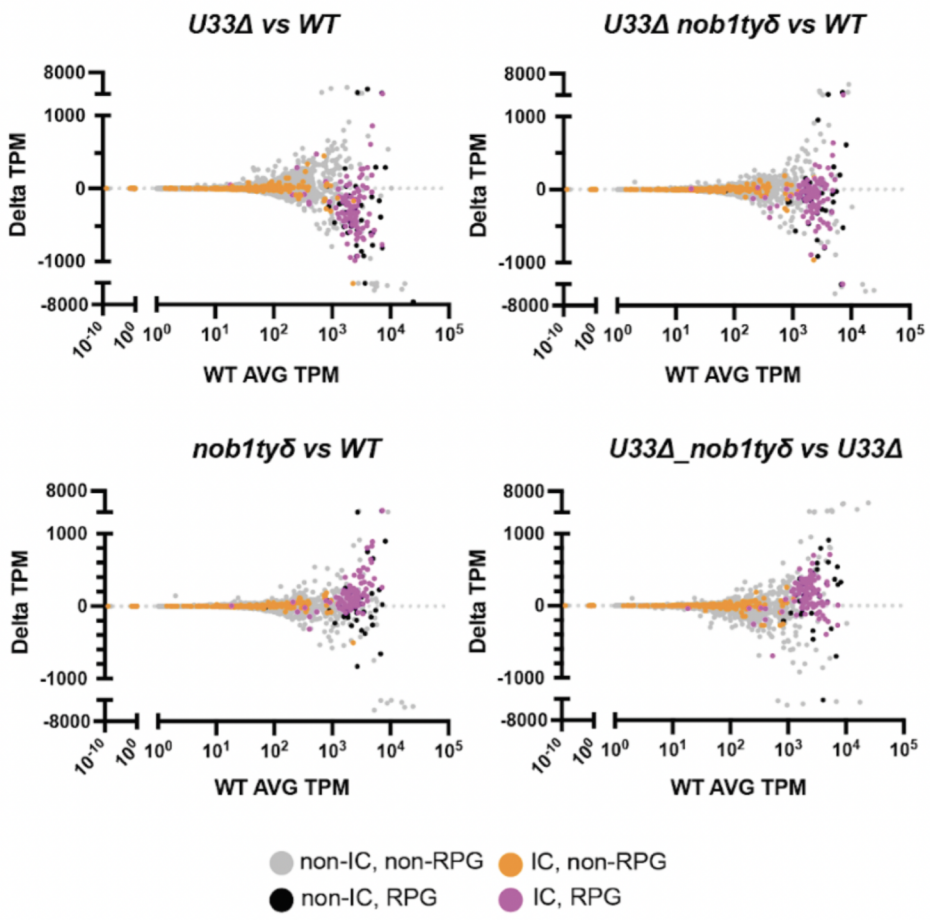


**Figure 11: *U33Δ* has a decreased trend in gene expression that is increased in *U33Δ nob1-Tyδ*.** Nob1-Tyδ causes changes in gene expression compared to both wild-type and *U33Δ*. Gene expression is measured by transcripts per million, comparing the change in each mutant to the average in wild-type. IC = intron containing. RPG = ribosomal protein gene.

# 3 - Prp43 provides a potential link between ribosome biogenesis and splicing

Next, we investigated the protein Prp43 as a possible mechanism for causing suppression of *U33Δ* via *nob1-Tyδ*. Although Nob1 has no direct link with splicing, Prp43 is involved in both the splicing cycle and rRNA processing with Nob1. Prp43 is a DEAH-box RNA helicase that catalyzes the removal of U2, U5, and U6 snRNPs from the splicing complex (Combs et al. 2006) and also acts with the G-patch protein Sqs1 to promote processing of 20S to 18S via Nob1 (Pertschy et al. 2009). We hypothesized that there could be an effect where Prp43 is sequestered by Nob1 into the rRNA processing pathway due to Nob1 malfunctioning from the Tyδ insert. In this case, the spliceosome would not be disassembled as readily by Prp43. This may allow more time for a mutant spliceosome to splice introns in essential mRNAs that the mutant BSL would otherwise reject.

To test this we induced overexpression of Prp43 via a high-copy plasmid in *U33Δ*, with and without *nob1-Tyδ*. With excess Prp43 in the cell, we expected the suppression effect could be negated as Prp43 could more readily disassemble mutant spliceosomes before they could splice. However, we saw that *nob1-Tyδ* continued to suppress *U33Δ* even with excess Prp43 (Figure 12). The excess Prp43 appeared not to affect the growth of the mutant at 37°C, so it is unlikely that a lack of Prp43 is responsible for *U33Δ* rescue by *nob1-Tyδ*.

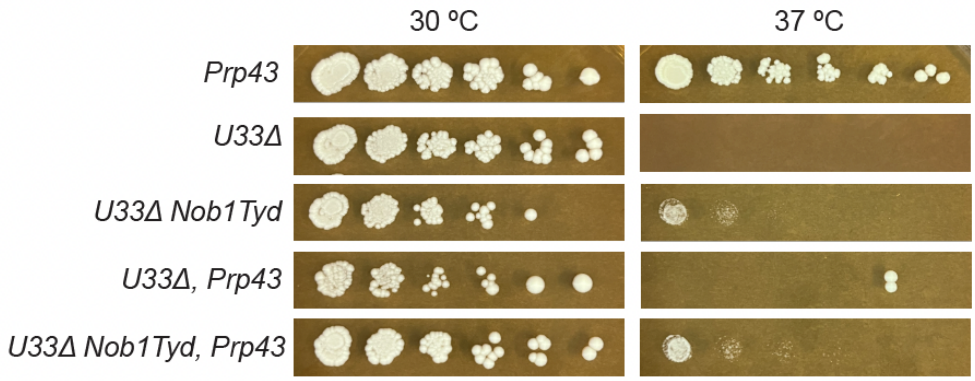


**Figure 12: Prp43 overexpression fails to negate *nob1-Tyδ*'s suppression of *U33Δ*.** Prp43 has no discernable influence on the growth of *U33Δ* at 37°C degrees, with or without *nob1-Tyδ*.

Since Prp43 works together with protein Sqs1 in stimulating the processing of 20S (Lebaron et al. 2009), we also tested whether deletion of Sqs1 would affect suppression. By deleting Sqs1, it would be prevented from assisting Prp43 in the rRNA maturation pathway, leading to Prp43 no longer being sequestered by *nob1-Tyδ*. We predicted this would have an effect similar to overexpressing Prp43. In this too, we did not see a reduction in suppression by *nob1-Tyδ*. Deletion of Sqs1 generally improves the mutants' growth at 37°C, but it does not appear to be a specific effect; all strains with *sqs1Δ* have slightly better growth at 37°C, regardless of the other mutations. With no clear mechanism that could directly interact with the spliceosome and Nob1, we decided to investigate whether the suppression could be related to the changes in the pre-mRNA pool.

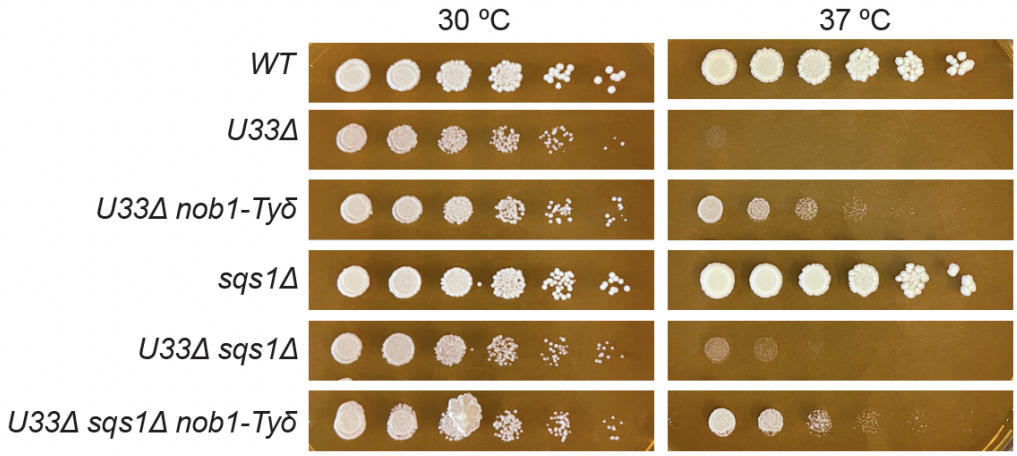


**Figure 13: Deletion of Sqs1 fails to suppress *U33Δ*.** Sqs1 deletion has a general positive effect on growth at 37°C, with *U33Δ sqs1Δ* and *U33Δ nob1-Tyδ sqs1Δ* growing slightly better than *U33Δ* and *U33Δ nob1-Tyδ* alone at 37°C. The deletion of *SQS1* does not counteract suppression by *nob1-Tyδ.*

# 4 - Manipulation of ribosomal protein gene expression can rescue splicing mutants

Previous work has shown that making changes in ribosomal protein gene (RPG) expression can rescue other temperature-sensitive splicing mutants (Munding et al. 2013). This suggests that if pre-mRNAs compete for limited splicing capacity, the competition is increased for impaired spliceosomes, so reducing the number of nonessential pre-mRNAs can increase splicing capacity. In *S. cerevisiae,* RPGs make up a highly significant part of the spliceosome's workload; more than a third of intron-containing genes are RPGs, and their mRNAs account for 90% of the spliceosomal load (M. Ares Jr, Grate, and Pauling 1999). In this previous study (Munding et al. 2013), temperature-sensitive mutations in snRNPs Prp11 and Prp4 were rescued by downregulating the ribosomal protein gene transcription factor

IFH1 via a galactose promoter. Using this system, IFH1 expression and therefore RPG pre-mRNA levels were significantly reduced when grown on glucose, and temperature-sensitive splicing mutants, *prp11-1* and *prp4-1*, were rescued (Figure 14).

Although suppression of specific splicing mutants was determined to be correlated with a processing defect of rRNA processing caused by Nob1, it was still unclear how the suppression functioned. There is no direct interaction between Nob1 and the spliceosome, and modifications to Prp43 expression did not affect suppression. We hypothesized there could be suppression due to how the Nob1 mutation could affect the pre-mRNA pool, and therefore the number of intron-containing transcripts the spliceosome must splice. As the analysis of splicing activity indicates, *nob1-Tyδ* does not appear to drastically change splicing compared to wild-type, so its mechanism is unlikely to be a direct effect targeting the splicing of specific pre-mRNAs. We hypothesized rescue of *U33Δ* is likely due to the changes in gene expression and therefore changes to the pre-mRNA pool and the splicing load. With changes to the pre-mRNA pool created by *nob1-Tyδ*, the compromised splicing machinery of mutants like U33Δ may have more opportunities to splice critical growth-limiting introns that otherwise remain unspliced.

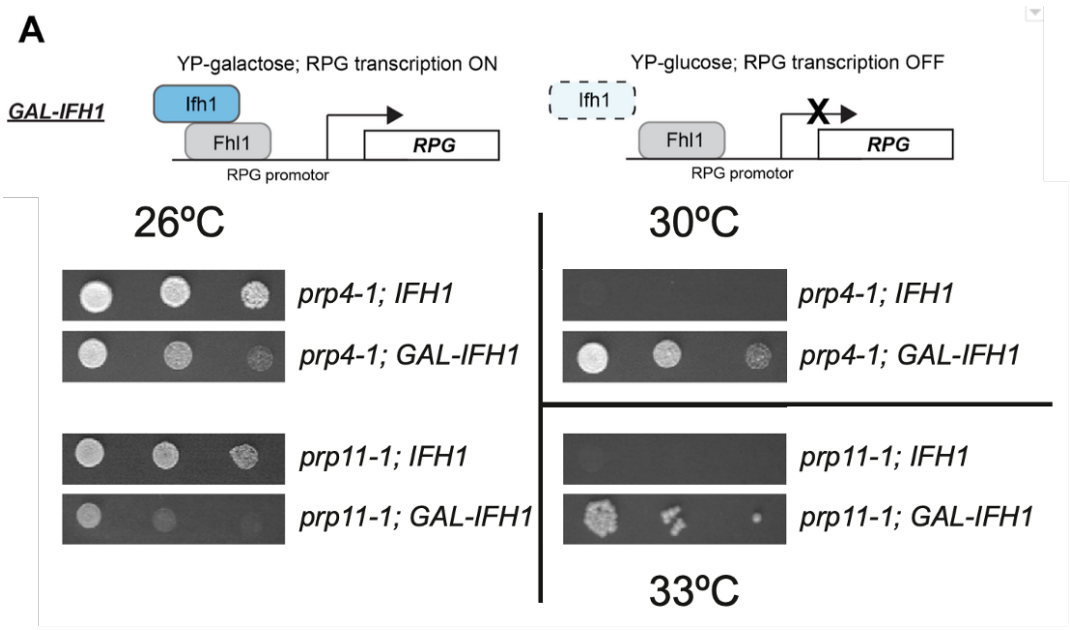


**Figure 14: Downregulation of ribosomal protein genes rescues mutations in other splicing factors (figure adapted from Munding et al. 2013).** Previous research shows suppression of temperature sensitive mutations in Prp4 and Prp11 by decreasing RPG expression.

We also tested whether using this same system to downregulate RPGs could rescue BSL mutants. We constructed a strain with U2 deletion covered by a plasmid and IFH1 under the control of a galactose promoter. When grown on glucose-containing media, some of the cold-sensitive BSL mutants, *A31G* and *C41U*, saw improved growth at 18°C (Figure 15). Some mutants grew worse when grown on galactose, indicating that overexpression of IFH1 can reduce growth for splicing mutants.

For the mutant *U33Δ*, downregulation of IFH1 did not improve growth (Figure 15). Since all the BSL mutants were rescued by *nob1-Tyδ* but not *GAL-IFH1*, these observations could indicate that splicing mutants may have unique selective effects and that not all splicing defects can be rescued by the same suppressor. Alternatively, the *U33Δ* mutation may make a

more severe defect than either *prp11-1* or *prp4-1*, and the suppression effect of IFH1 downregulation may not be sufficient. Either way, mutant spliceosomes may be leaving critical introns unspliced, but which introns that are going unspliced could be different depending on the exact mutants and the non-permissive temperatures they are tested at. We sought to explore this further by testing whether other methods of reducing competition for a compromised spliceosome could rescue growth.

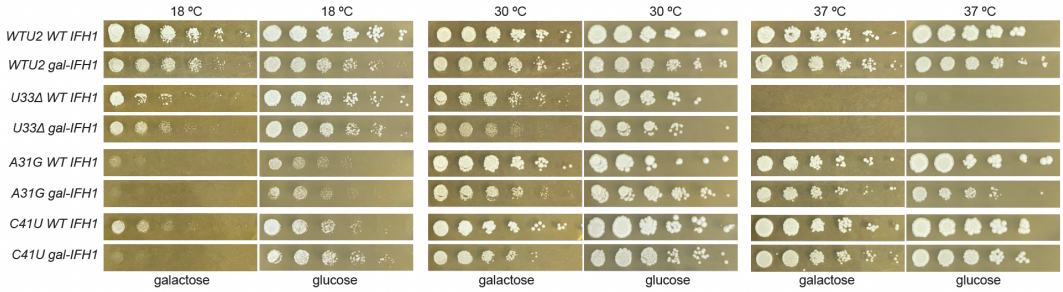


**Figure 15: Downregulating RPGs via *IFH1* rescues cold-sensitive BSL mutants.** *A31G* and *C41U* show improved growth at 18°C.

# 5 - Manipulation of the splicing load in other ways can rescue splicing mutants

Though the bulk of the spliceosome's workload in *S. cerevisiae* is RPG pre-mRNAs, there are other intron-containing pre-mRNAs unrelated to ribosome biogenesis. To reduce the splicing load without influencing RPG expression, we attempted a different approach by targeting highly expressed and efficiently spliced intron-containing genes that are not involved in ribosome biogenesis, as determined by our RNA sequencing data. *HNT1*, *ECM33*, and *UBC4* are the three most highly expressed intron-containing non-RPG genes in

*S. cerevisiae*, making up a significant portion of the spliceosome's workload. We generated a strain with the introns deleted in these three genes, resulting in mRNA that produces the same protein product but does not require splicing. We combined this triple-intron deletion (*HEU*Δi) with *U33Δ*, and the triple-intron deletion dramatically increased the growth of *U33Δ* at 37°C to practically the same as wild-type. Even single gene intron deletions were shown to rescue *U33Δ* growth, with *ubc4Δi* resulting in the strongest rescue, corresponding to its higher expression. Additionally, the triple-intron deletion rescued the temperature sensitive *prp11-1* mutant, previously shown to be rescued by IFH1 downregulation. This finding provides additional evidence that reducing the splicing load by deleting introns in highly competitive pre-mRNAs can rescue splicing mutants and the reduction does not have to involve RPGs.

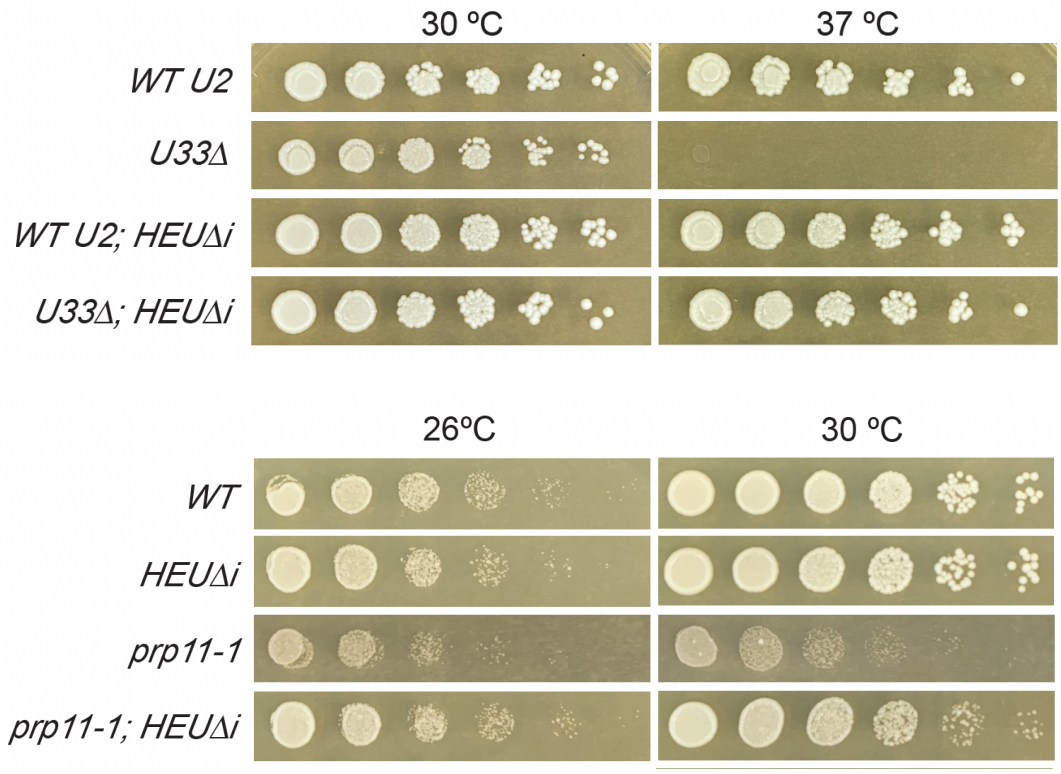


**Figure 16: Deleting highly spliced non-RPG introns rescues *U33Δ* and *prp11-1*.** *HNT1*, *ECM33*, and *UBC4* are normally highly spliced, and deletion of their introns reduces competition for the spliceosome.

Next, we sought to alter the apparent splicing capacity from a different angle. By utilizing the autoregulated splicing mechanism of Prp5, we tested whether we could rescue *U33Δ* by increasing the cell's splicing capacity. Although introns are sometimes considered non-coding regions of genes that are transcribed into RNA but later removed during the splicing process, introns can contain important regulatory elements that affect gene expression and function. Prp5 is a DEAD-box protein that functions in spliceosome assembly by removing Cus2 (Perriman and Ares 2010), and its start codon is contained within its intron

(Miura et al. 2006). This protein's pre-mRNA contains an intron that overlaps the protein coding region so that its removal inactivates the mRNA. The intron includes the start codon and must be retained for Prp5 to function, with the deletion of the intron being lethal (Karaduman et al. 2017). Because Prp5 is essential for splicing, this creates an autoregulation feature where an abundance of Prp5 results in its own pre-mRNAs being more highly spliced. This, in turn, lowers the amount of functional Prp5 and so reduces the splicing level.

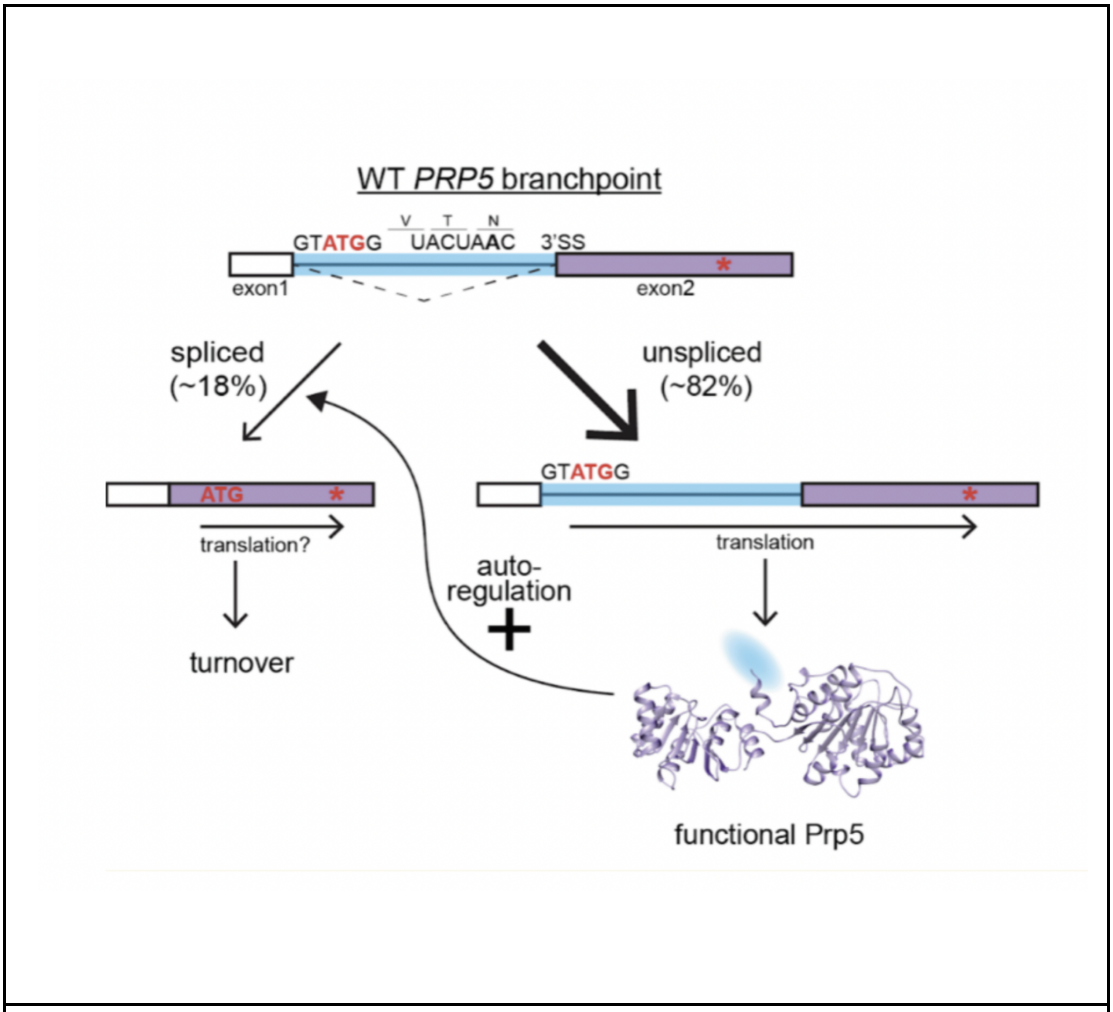


**Figure 17: Prp5 is only functional when its intron is retained, facilitating autoregulation of splicing.** The start codon is within the intron, resulting in functional Prp5 protein only when unspliced.

We created a strain featuring a mutant branchpoint (AACAAAU instead of UACUAAC) in Prp5's pre-mRNA intron (*PRP5-BP*), preventing it from being spliced while maintaining the ORF and amino acid sequence. This presumably creates an overabundance of Prp5 as it will continue to be functional even when the increased splicing capacity would otherwise signal its reduced expression. When combined with *U33Δ*, we could see that mutating *PRP5's* branchpoint dramatically rescues *U33Δ's* temperature-sensitive growth defect. This mutant also rescued other splicing mutants, including other BSL mutants and *prp11-1*. Combined with rescue by the triple intron deletion, this rescue suggests that changing the pre-mRNA pool or spliceosome's capacity can neutralize the effect of a compromised spliceosome.

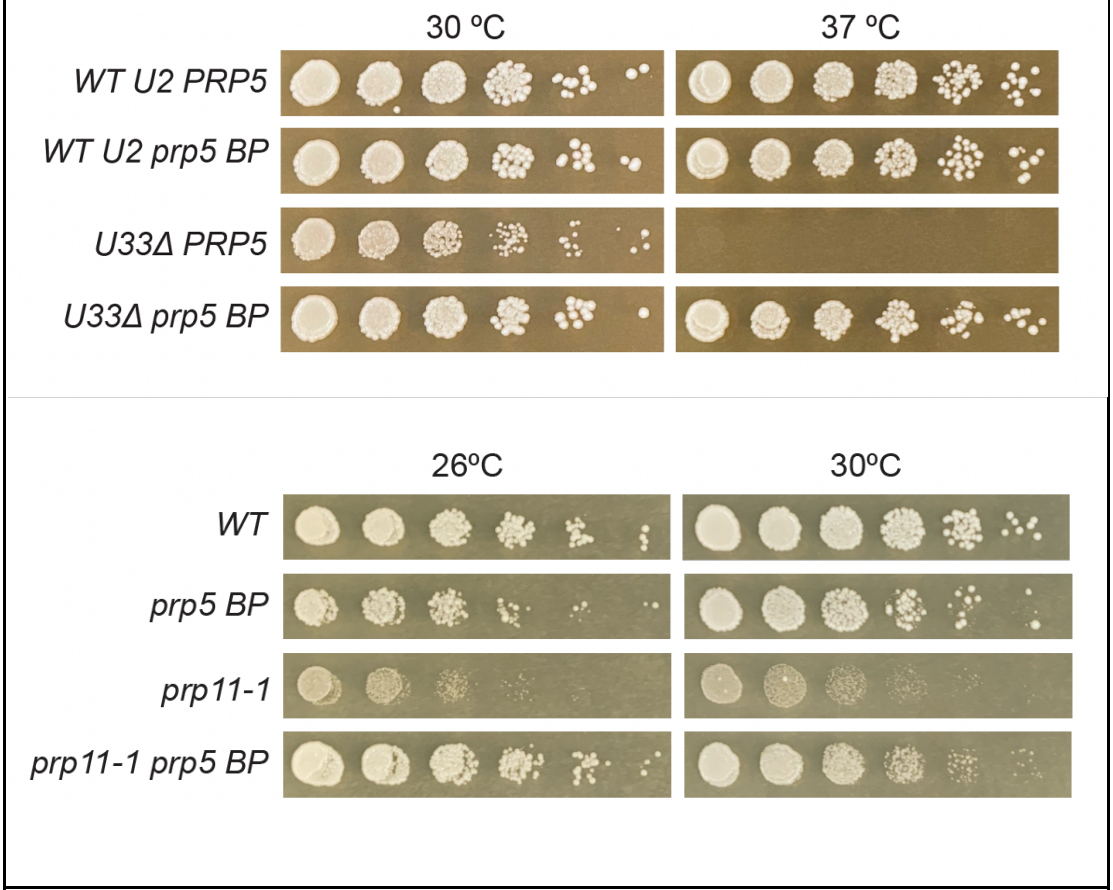


**Figure 18: A mutation in Prp5's branch point enables increased splicing capacity and rescues *U33Δ* and *prp11-1*.** The mutant *PRP5-BP* increases Prp5 expression and results in rescued growth for *U33Δ* at 37 and improved growth for *prp11-1*.

# 6: Discussion

We initially set out to characterize the suppressor of a BSL mutation. Such suppressors can illuminate protein and RNA interactions within the spliceosome, revealing key functions of splicing components. The characterization of *nob1-Tyδ* revealed that this suppressor has no direct interaction with the spliceosome machinery but instead changes the landscape the spliceosome operates in by altering the splicing load of pre-mRNAs.

The insertion of a Ty delta element in the C-terminal end of Nob1-Tyδ affects how it processes pre-rRNA but has no clear direct link between this process and splicing. rRNA processing of 20S RNA was reduced in the mutant, resulting in the accumulation of 20S, but this processing defect has no direct relation to splicing. Investigating the potential factor that could link the two, Prp43, found no effect on suppression. Instead of finding a direct mechanistic link between rRNA processing and splicing, we turned towards a system-wide approach.

We hypothesize that when a cell has a defect in its splicing machinery, such as *U33Δ*, it cannot splice all the necessary pre-mRNAs needed for survival. Less competitive pre-mRNAs remain unspliced; if these are essential for growth, the cell fails to survive. In the case of *U33Δ,* it is thought that such a splicing defect is due to the BSL being too unstable to remain in contact with the branchpoint long enough to accept branchpoints, especially if the branchpoint sequence is uncommon.

For *nob1-Tyδ* to rescue this defect without directly interfering with the splicing machinery, it must change the pool of pre-mRNAs needed to be spliced for survival. RNA sequencing showed that *nob1-Tyδ* changes gene expression, reversing the decrease in gene expression in *U33Δ*. Although this effect of upregulating RPGs is contrary to what previous

studies have shown regarding malfunctioning ribosomal biogenesis, and the reason for this remains unknown, this change does indicate the change in gene expression could be responsible for the suppression of *U33Δ*. *nob1-Tyδ* rescues the splicing defect in *U33Δ*, supporting our hypothesis that *nob1-Tyδ* signals a shift in gene expression that leads to a decreased splicing load and enhanced overall splicing efficiency. An increase in splicing efficiency is not seen with wild-type U2, so it is unlikely *nob1-Tyδ* is directly affecting splicing efficiency. Splicing efficiency is improving because of the changes to gene expression, which can be seen in *nob1-Tyδ* with wild-type U2. Previous work has shown that when deprived of pre-mRNA with consensus branchpoints, the spliceosome will splice less competitive introns (Talkish et al. 2019). So we hypothesize that the changes to gene expression by *nob1-Tyδ* give *U33Δ* the ability to splice these less competitive introns critical for growth at 37℃. Although the way *nob1-Tyδ* rescues is still unclear as it causes an overall increase in gene expression, particularly RPGs, it does signify that manipulating the pre-mRNA pool can rescue splicing mutants.

Increasing the splicing capacity or decreasing the splicing load were both able to rescue *U33Δ*. Deletion of the introns in the three most highly spliced non-RPG genes dramatically rescued *U33Δ*, as did removing Prp5's ability to autoregulate to effectively increase splicing capacity. Restoration of growth powerfully demonstrates how splicing mutants can be rescued not by direct interaction with other splicing factors but by changing the landscape of pre-mRNA within the cell.

It is important to note that rescue by altering the pre-mRNA pool is not a universal rescue for all splicing mutants. *IFH1* downregulation fails to rescue *U33Δ,* and *nob1-Tyδ* fails to rescue *prp11-1*, though *PRP5-BP* and the triple intron deletions were able to rescue both *prp11-1* and BSL mutations. Each of these mutants causes splicing defects, resulting in some

pre-mRNAs not getting spliced. This raises the question; which essential pre-mRNAs are not getting spliced? Our idea is that these “biggest losers” of pre-mRNA splicing are vital, and yet the defective spliceosome does not have time to splice them, causing cell death at each mutant’s non-permissive temperatures. What these specific pre-mRNAs could be remains unknown, but it’s probable they are different for each splicing mutant. This difference leads to the difference in working suppressors; for some, the suppressor could not be enough to allow to spliceosome to get to the biggest loser pre-mRNA, and in some, the suppressor mutation could be too drastic for the cell to function with both spliceosome mutation and suppressor mutation. These differences in rescue indicate that the balance between splicing load and splicing capacity is highly tuned.

The study of splicing has been a major focus of genetics, biochemistry, and structural biology. While much has been learned about the mechanics of splicing and its direct protein and RNA interactions, we still lack a comprehensive understanding of how splicing is integrated into other cellular processes. It is clear that splicing is influenced not only by its structure and interactions but also by its workload and capacity. The spliceosome exists in a complex and dynamic landscape that is still not fully understood. Further research is needed to fully unravel the interplay between splicing and other cellular processes and gain a deeper understanding of the biological significance of splicing regulation.

# Materials and Methods

**Growth and Strains**

Yeast strains were grown at 30°C on YEPD (2% dextrose, 2% peptone, 1% yeast extract) except where noted. Transformations were done according to standard methods (Rose, Winston, and Hieter 1990). Strains are listed in Table 1. BY4743 U2 deletion strain, *nob1-Tyδ* strain, Nob1 truncation, and *prp11-1* were all constructed using CRISPR/Cas9, described below. All other strains featuring both a mutant and a potential suppressor were created via crossing.

**RNA Isolation**

RNA was extracted as described in (Manuel Ares 2012). Cells were grown to within 0.1 $OD_{600}$ of 0.5, and then temperature shifted to 37°C for one hour. Cells were harvested to an equivalent amount of 10mL at $OD_{600}$ 0.5. 50uL of pre-frozen *S. pombe* at 0.4 $OD_{600}$ was used as a spike-in. RNA was analyzed using Aligent 2100 Bioanalyzer, Nano 6000.

**RNA sequencing and analysis**

10 samples were sequenced by Fulgent, 2 replicates each of *U33Δ NOB1*, *U33Δ nob1-Tyδ*, *U33Δ G32A* (not discussed in this thesis) and wild-type. Total RNA was provided and Fulgent prepared the libraries from poly(A) selected RNA. Libraries were sequenced (150 pair-end) using an Illumina HiSeq4000. Gene expression analysis was done with Kallisto to calculate transcripts per million (TPM_. Cutadapt was used to trim the reads to 120x120. Reads were aligned to SacCer3_ares_v11.

Genes involved in meiosis or relating to mating type were filtered to account for the different mating types used. Pre-mRNA transcripts containing two introns were filtered. Gene expression was analyzed by comparing TPMs to show the difference in expression relative to

how abundant a transcript is in the cell. Average TPM of the wild-type was plotted (x-axis) in comparison to the difference in TPM of each mutant (y-axis).

Sol Katzman performed splicing efficiency analysis. Splicing efficiency was calculated for each intron by counting splice junction (SJ) crossing reads and reads that cross unspliced splice sites (EI and IE) at either end of the intron (5'SS and 3'SS). Efficiency is given by the % Spliced, which is the number of SJ reads divided by the sum of the SJ reads and the number of EI + IE reads divided by 2 X100. Splicing efficiencies were compared between samples via X/Y scatter plots.

**DNA sequencing and analysis**

gDNA was extracted from 10 wild type spores and 10 suppressor spores. Equal molar amounts of each spore's DNA were pooled to create two samples for sequencing. Sequencing was performed by the genomics labs at UC Berkeley. 75 pair-end sequencing was performed on an Illumina MiSeq instrument. John Paul Donohue performed the analysis, using MIRA to assemble the sequences. The genome was assembled, and differences were found between the two samples.

**CRISPR/Cas9**

CRISPR/Cas9 was performed as described in (Talkish et al. 2019). Guide RNAs were first annealed and then ligated into the BaeI-digested plasmid p416-TEF1p-Cas9-NLS-crRNA-BaeI. All the strains had plasmids with their respective gRNA plasmids co-transformed with their rescue fragments and selected for on SCD-Ura media. Colony PCR using primers flanking the target site was used to confirm successful integration and then sequenced at the UC Berkeley Sequencing Center.

BY4743 U2 deletion strain was created using oligonucleotides 3330 and 3331 for PCR (Table 2) using pFA6a–natNT2 (Janke et al. 2004). Oligos 2986 and 2987 were used to create the

guide RNA fragment. After the CRISPR transformation and selecting, the diploid strain was then transformed with a U2 plasmid, then sporulated and dissected to select for haploid spores with matching genotypes to BY4741 and BY4742 and featuring *LSR1Δ::nat*.

The *nob1-Tyδ* mutation was recreated in the BY4742 U2 deletion strain with *U33Δ*. Oligonucleotides 3135 and 3363 were used to create a PCR rescue fragment, using the original suppressor strain's genome as a template. This rescue fragment resulted in a product identical to the original Tyδ's sequence. Oligonucleotides 3228 and 3229 were used, encoding a guide RNA targeting *NOB1*. After transformation, cells were selected for at 37℃ for suppression. PCR using primers flanking the Tyδ was used to confirm successful integration.

The *NOB1* truncation strain was created using the same plasmid as used in *nob1-Tyδ* CRISPR, while oligonucleotides 3230 and 3231 were used to create the rescue fragment. This rFrag introduces two stop codons to truncate Nob1 after position 432, where the Tyδ begins in the original suppressor strain.

The *prp11-1* strain was created in BY4742 using oligonucleotides 3222 and 3223 for the gRNA. The rescue fragment was created using oligonucleotides 3224 and 3225.

Table 1: Strains

| STRAIN | GENOTYPE | SOURCE |
|---|---|---|
| MS22 | *MATα his3Δ1 leu2Δ0 lys2Δ0 ura3Δ0 U2Δ::nat (p URA3-WT U2)* | BY4743 |
| MS23 | *MATa his3Δ1 leu2Δ0 lys2Δ0 ura3Δ0 U2Δ::nat (p URA3-WT U2)* | BY4743 |
| MS11 | *MATα his3Δ1 leu2Δ0 ura3Δ0 met15Δ0* | MS22, |

| | | |
|---|---|---|
| | *U2Δ::nat Nob1-Tyδ (p URA3-WT U2)* | CRISPR/Cas9 Nob1-Tyδ |
| KY6 | *PRP5-BP his3Δ1 leu2Δ0 met15Δ0 ura3Δ0 MATa* | Kyle Tanguay, Ares Lab |
| MS7 | *PRP5-BP U2Δ::nat MATa met15Δ0 his3Δ2 leu2Δ0 ura3Δ0 p(URA3 WT U2)* | Spore from KY6 x MS22 |
| MS10 | *prp11-1 MATα his3Δ1 leu2Δ0 metΔ0 ura3Δ0* | BY4742, CRISPR/Cas9 Prp11-1 |
| HEUΔi (MS12) | *Hnt1Δi Ubc4Δi Ecm33Δi MATa his3Δ1 leu2Δ0 met15Δ0 ura3Δ0* | Haller Igel, Ares Lab |
| MS32 | *Hnt1Δi Ubc4Δi Ecm33Δi U2Δ::nat (pURA3-WT U2)* | Spore from MS12 x MS22 |
| MS43 | *Nob1-trunc MATa his3Δ1 leu2Δ0 lys2Δ0 ura3Δ0 U2Δ::nat (p LYS-WT U2)* | MS23, CRISPR/Cas9 Nob1-trunc |
| EMY2 | *BY4741, k-HIS3:GAL1-IFH1* | Lisa Munding, Ares Lab |
| SRY11-1d | *MATα prp11-1 ade2- his- his4- leu2- tyr1- ura3-52* | Lisa Munding, Ares Lab |
| EMY4 | *prp11-1, k-HIS3:GAL1-IFtH1* | Lisa Munding, Ares Lab, spore from EMY2 x SRY11-1d |
| MS37 | *k-HIS3:GAL1-IFH1, U2Δ::nat, (p URA-WT U2)* | Spore from EMY2 x MS22 |
| MS8 | *PRP5-BP prp11-1 his3Δ1 leu2Δ0 ura3Δ0* | Spore from KY6 x MS10 |
| MS11 | *prp11-1 HNT1Δi ECM33Δi UCB4Δi MATa his3Δ1 leu2Δ0 ura3Δ0 met15Δ0* | Spore from MS10 x HEUΔi |

| | | |
|---|---|---|
| MS22 - Prp43 | *MATα his3Δ1 leu2Δ0 lys2Δ0 ura3Δ0 U2Δ::nat (p LYS-U2, p-LEU PRP43)* | |
| MS56 | *Sqs1d::KAN* – in BY4741 (a) *his3Δ1 leu2Δ0 met15Δ0 ura3Δ0* | |
| MS67 | *Sqs1d::KAN U2Δ::nat (p URA3-WT U2)* | Spore from MS22 x MS 56 |

Table 2: Oligos

| Oligo | Purpose | Sequence (5'-3') |
|---|---|---|
| 3330 | *U2Δ::Nat* rFrag- F (S1) | TTCATCGATGAGTACTTTACTTGT TATCAGATTTATTCATTTTGTTTC TACTTGTTTTTTTTTTAAATCCCC CGTACGCTGCAGGTCGAC |
| 3331 | *U2Δ::Nat* rFrag - R (S2) | TTCTTCAAATCCCTCCAAAAAAA ACGCCTCTATGACATAGGCGGTT AATAAAACTGGCCTTGAAACAAC AGATCGATGAATTCGAGCTCG |
| 3135 | *Tyδ* for *NOB1* CRISPR rFrag - F | CACTGGTTCATTGGGTGTAGAAG |
| 3363 | *Tyδ* for *NOB1* CRISPR rFrag - R | TTTTGGAACTGTTGACGTACCTTC CCTTACCAATGCGGACGTTATGC TGCTTCAAACCAGTAATTGCAAA TGGA |
| 3230 | *nob1-trunc* rFrag - F | GATTGGTGGCGGTTCTGCGGATA ACTATATTTCTTAATAAGCAATT ACTGGGTTGAAGCAGCATAACGT CCGCATTGGTAAGGGAAGGTA |
| 3231 | *nob1-trunc* rFrag - R | TACCTTCCCTTACCAATGCGGAC GTTATGCTGCTTCAACCCAGTAA TTGCTTATTAAGAAATATAGTTA |

| | | |
|---|---|---|
| | | TCCGCAGAACCGCCACCAATC |
| 3224 | *prp11-1* rFrag - F | GAAAATAGTGTCGATAGCGATGA TAAGGCTAAAGTCCCTCTTCTCA TTAGAATTGTATCTGGTTTAGAA CTATCAGATACCAAACAGAAG |
| 3225 | *prp11-1* rFrag - R | CTTCTGTTTGGTATCTGATAGTTC TAAACCAGATACAATTCTAATGA GAAGAGGGACTTTAGCCTTATCA TCGCTATCGACACTATTTTC |
| 2986 | U2 gRNA - F | AGTGAAAGATAAATGATCTCCCG TCCATTTTATTATTTGTTTTAGAG CTAGAAATA |
| 2987 | U2 gRNA - R | TATTTCTAGCTCTAAAACAAATA ATAAAATGGACGGGAGATCATTT ATCTTTCACT |
| 3228 | Nob1 gRNA - F | AGTGAAAGATAAATGATCTTTCT CCATTTGCAATTACTGTTTTAGAG CTAGAAATA |
| 3229 | Nob1 gRNA - R | TATTTCTAGCTCTAAAACAGTAA TTGCAAATGGAGAAAGATCATTT ATCTTTCACT |
| 3222 | Prp11 gRNA - F | AGTGAAAGATAAATGATCCTAAA GTCCCTCCTCTCATTGTTTTAGAG CTAGAAATA |
| 3223 | Prp11 gRNA - R | TATTTCTAGCTCTAAAACAATGA GAGGAGGGACTTTAGGATCATTT ATCTTTCACT |

# References


Ameismeier, Michael, Jingdong Cheng, Otto Berninghausen, and Roland Beckmann. 2018. "Visualizing Late States of Human 40S Ribosomal Subunit Maturation." *Nature* 558 (7709): 249–53.

Ares, Manuel. 2012. "Isolation of Total RNA from Yeast Cell Cultures." *Cold Spring Harbor Protocols* 2012 (10): 1082–86.

Ares, M., Jr, L. Grate, and M. H. Pauling. 1999. "A Handful of Intron-Containing Genes Produces the Lion's Share of Yeast mRNA." *RNA* 5 (9): 1138–39.

Combs, D. Joshua, Roland J. Nagel, Manuel Ares Jr, and Scott W. Stevens. 2006. "Prp43p Is a DEAH-Box Spliceosome Disassembly Factor Essential for Ribosome Biogenesis." *Molecular and Cellular Biology* 26 (2): 523–34.

Cruz, Jesús de la, Fernando Gómez-Herreros, Olga Rodríguez-Galán, Victoria Begley, María de la Cruz Muñoz-Centeno, and Sebastián Chávez. 2018. "Feedback Regulation of Ribosome Assembly." *Current Genetics* 64 (2): 393–404.

Fatica, Alessandro, Marlene Oeffinger, Mensur Dlakić, and David Tollervey. 2003. "Nob1p Is Required for Cleavage of the 3′ End of 18S rRNA." *Molecular and Cellular Biology* 23 (5): 1798–1807.

Janke, Carsten, Maria M. Magiera, Nicole Rathfelder, Christof Taxis, Simone Reber, Hiromi Maekawa, Alexandra Moreno-Borchart, et al. 2004. "A Versatile Toolbox for PCR-Based Tagging of Yeast Genes: New Fluorescent Proteins, More Markers and Promoter Substitution Cassettes." *Yeast* 21 (11): 947–62.

Karaduman, Ramazan, Sittinan Chanarat, Boris Pfander, and Stefan Jentsch. 2017. "Error-Prone Splicing Controlled by the Ubiquitin Relative Hub1." *Molecular Cell* 67 (3): 423–32.e4.

Lebaron, Simon, Christophe Papin, Régine Capeyrou, Yan-Ling Chen, Carine Froment, Bernard Monsarrat, Michèle Caizergues-Ferrer, Mikhail Grigoriev, and Yves Henry. 2009. "The ATPase and Helicase Activities of Prp43p Are Stimulated by the G-Patch Protein Pfa1p during Yeast Ribosome Biogenesis." *The EMBO Journal* 28 (24): 3808–19.

Miura, Fumihito, Noriko Kawaguchi, Jun Sese, Atsushi Toyoda, Masahira Hattori, Shinichi Morishita, and Takashi Ito. 2006. "A Large-Scale Full-Length cDNA Analysis to Explore the Budding Yeast Transcriptome." *Proceedings of the National Academy of Sciences of the United States of America* 103 (47): 17846–51.

Munding, Elizabeth M., Lily Shiue, Sol Katzman, John Paul Donohue, and Manuel Ares Jr. 2013. "Competition between Pre-mRNAs for the Splicing Machinery Drives Global Regulation of Splicing." *Molecular Cell* 51 (3): 338–48.

Perriman, Rhonda, and Manuel Ares Jr. 2010. “Invariant U2 snRNA Nucleotides Form a Stem Loop to Recognize the Intron Early in Splicing.” *Molecular Cell* 38 (3): 416–27.

Pertschy, Brigitte, Claudia Schneider, Marén Gnädig, Thorsten Schäfer, David Tollervey, and Ed Hurt. 2009. “RNA Helicase Prp43 and Its Co-Factor Pfa1 Promote 20 to 18 S rRNA Processing Catalyzed by the Endonuclease Nob1.” *The Journal of Biological Chemistry* 284 (50): 35079–91.

Plaschka, Clemens, Pei-Chun Lin, Clément Charenton, and Kiyoshi Nagai. 2018. “Prespliceosome Structure Provides Insights into Spliceosome Assembly and Regulation.” *Nature* 559 (7714): 419–22.

Rose, Mark David, Fred Marshall Winston, and Philip Hieter. 1990. *Methods in Yeast Genetics: A Laboratory Course Manual*. Cold Spring Harbor Laboratory Press.

Talkish, Jason, Haller Igel, Rhonda J. Perriman, Lily Shiue, Sol Katzman, Elizabeth M. Munding, Robert Shelansky, John Paul Donohue, and Manuel Ares Jr. 2019. “Rapidly Evolving Protointrons in Saccharomyces Genomes Revealed by a Hungry Spliceosome.” *PLoS Genetics* 15 (8): e1008249.

Yan, D., and M. Ares Jr. 1996. “Invariant U2 RNA Sequences Bordering the Branchpoint Recognition Region Are Essential for Interaction with Yeast SF3a and SF3b Subunits.” *Molecular and Cellular Biology* 16 (3): 818–28.

Zhang, Zhenwei, Cindy L. Will, Karl Bertram, Olexandr Dybkov, Klaus Hartmuth, Dmitry E. Agafonov, Romina Hofele, et al. 2020. “Molecular Architecture of the Human 17S U2 snRNP.” *Nature* 583 (7815): 310–13.